Journal of Materials Chemistry C



PAPER

View Article Online



Cite this: J. Mater. Chem. C. 2022. 10.13974

Simultaneous reinforcement of the electrical and mechanical properties of carbon nanotube fibers by using a natural cross-linkable thermosetting polymer†

Hyun Jun Cho, Da Chul-Jun Yoon, Junbeom Park, Hansol Kang, Insik In, Dc Seung Min Kim b and Young-Kwan Kim **

A simple and efficient reinforcement strategy for the mechanical and electrical properties of carbon nanotube (CNT) fibers is developed by using natural urushiol as an eco-friendly cross-linking agent. This strategy is a sequential process including infiltration and cross-linking of urushiol onto CNT fibers. Based on this process, the tensile strength (430 \pm 20 MPa), modulus (8.6 \pm 1.0 GPa), toughness (12.7 \pm 1.3 MJ m⁻³), and electrical conductivity (1616 \pm 115 S cm $^{-1}$) of CNT fibers increase to 1.32 \pm 0.01 GPa, 37.0 \pm 2.1 GPa, 31.1 \pm 2.6 MJ m $^{-3}$, and 4053 \pm 200 S cm $^{-1}$ with the photochemical cross-linking process and to 0.92 \pm 0.09 GPa, 21.3 \pm 3.9 GPa, 20.5 \pm 2.3 MJ m $^{-3}$, and 7430 \pm 447 S cm $^{-1}$ with the thermal crosslinking process, respectively.

Received 21st March 2022, Accepted 22nd July 2022

DOI: 10.1039/d2tc01139e

rsc.li/materials-c

^a Department of Chemistry, Dongguk University-Seoul campus, 30 Pildong-ro, Jung-gu, Seoul 04620, Republic of Korea. E-mail: kimyk@dongguk.edu

- ^b Institute of Advanced Composite Materials, Korea Institute of Science and Technology (KIST), Wanju-gun, Jeonbuk 55324, Republic of Korea
- ^c Department of Polymer Science and Engineering, Korea National University of Transportation, 50 Daehak-ro, Chungju-si, Chungbuk 27469, Republic of Korea † Electronic supplementary information (ESI) available: Additional mechanical and electrical characterization results to reveal the reinforcement effect of urushiol on CNT fibers. See DOI: https://doi.org/10.1039/d2tc01139e



Young-Kwan Kim

Prof. Young-Kwan Kim received his PhD in chemistry at Korea Advanced Institute of Science and Technology in 2012 and worked as a postdoctoral fellow at Seoul National University and the University of Massachusetts, Amherst. In 2015, he joined the Carbon Composites Research Center at Korea Institute of Science and Technology as a Senior Researcher. Since 2019, he has been working as an assistant professor

Department of Chemistry at Dongguk University. His research interests include the synthesis, surface functionalization, nanohybridization and macroscopic assembly of carbon based nanomaterials for development of bioanalytical platforms and high-performance nanocomposites.

Introduction

Carbon nanotubes (CNTs) have attracted much attention from various research fields owing to their unique and excellent chemical stability, and thermal, mechanical and electrical properties. For their practical applications in electrical conductor, automobile, defence, and aerospace industries, macroscopic assembly of CNTs into a fibrous structure is an essential step while maintaining the intrinsic properties of individual CNTs.² Therefore, there have been many efforts to efficiently assemble CNTs into a fibrous structure, and the fibrous spinning techniques can be classified into direct spinning from a vertical chemical vapour deposition (CVD) reactor with floating metallic catalysts,³ liquid crystal spinning of the highly concentrated dope of CNTs in super acids,4 and forest spinning from a vertically grown array of CNTs on a substrate.5

Among these spinning methods, direct spinning is particularly promising based on its compatibility with large-scale and continuous production of CNT fibers.⁶ However, directly-spun CNT fibers have failed to re-enact the electrical and mechanical properties of individual CNTs owing to the amorphous carbon layer, poor alignment, and porous structures which lower the efficiency of load and electron transfer process.7 To improve the performance of CNT fibers, numerous attempts have been made including purification, roll-to-roll pressing,8 densification with super acids,9 incorporation of metallic nanoparticles, 10 and chemical cross-linking. 11 Although these approaches have shown promise for reinforcement of CNT fibers, the simultaneous enhancement of their electrical and mechanical properties remained a challenging issue because they

require dangerous super acids, multi-step surface modifications, and expensive equipment.

In this regard, the infiltration and carbonization of polymers onto CNT fibers is a simple and promising approach to simultaneously enhance their mechanical and electrical properties through filling the voids of CNT fibers with structurally analogous graphitic materials. 12,13 Ryu et al. showed that the mechanical and electrical properties of CNT fibers can be concurrently improved by infiltration and subsequent carbonization of polydopamine which converted it into a N-doped graphitic structure on the surface of CNT fibers. 12 We have reported that the resorcinol-formaldehyde (RF) resin can be efficiently infiltrated into CNT fibers and then carbonized with improvement of their electrical and mechanical properties by the alignment and densification effect. 13 These studies suggested that the rational selection of polymeric materials is a key step to efficiently improve the performance of CNT fibers. The requirements of potential polymeric materials for this purpose are cost-effectiveness, sustainability, high affinity toward the surface of CNT fibers, and low carbonization temperatures.

Urushiol, an oriental lacquer, is a traditional natural coating material and has been extensively utilized for wood and paper substrates.¹⁴ Urushiol is the main component of the sap of the lacquer tree, and it has an interesting chemical structure composed of a catechol unit and long hydrocarbon chains with unsaturated bonds (Fig. 1a). 15 The catechol unit can provide high affinity to CNT fibers, 16 and the unsaturated hydrocarbon chains can form a cross-linked polymeric network with CNT fibers by thermal and photochemical treatments. 17,18 In addition, it is an eco-friendly, natural, carbonizable, and readily available material from the sap of lacquer trees. 19 Based on these features, we hypothesized that urushiol could be a promising candidate for simultaneous enhancement of the mechanical and electrical properties of CNT fibers.

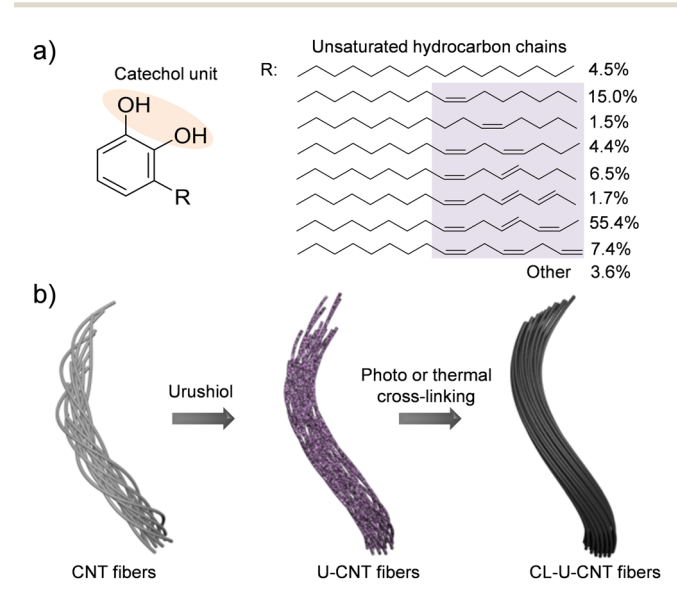


Fig. 1 (a) Chemical structure of urushiol and (b) a schematic diagram of urushiol infiltration into CNT fibers and their subsequent the photochemical and thermal cross-linking processes

Herein, we demonstrate the reinforcement of CNT fibers by using urushiol as an interfacial binder to interlock CNT bundles consisting of CNT fibers. Urushiol was infiltrated into CNT fibers, and the resulting urushiol infiltrated CNT (U-CNT) fibers were treated with UV irradiation or at an elevated temperature for their cross-linking (Fig. 1b). By urushiol infiltration and photochemical cross-linking, the tensile strength, modulus, toughness, and electrical conductivity of CNT fibers increased from 430 \pm 20 MPa, 8.6 \pm 1.0 GPa, 12.7 \pm 1.3 MJ m⁻³, and 1616 \pm 115 S cm⁻¹ to 1.32 \pm 0.01 GPa, 37.0 \pm 2.1 GPa, 31.1 \pm 2.6 MJ m⁻³, and 4053 \pm 200 S cm⁻¹, respectively. Likewise, the thermal treatment of U-CNT fibers also showed a considerable increase in these values to 0.92 \pm 0.09 GPa, 21.3 \pm 3.9 GPa, 20.5 \pm 2.3 MJ m⁻³, and 7430 \pm 447 S cm⁻¹, respectively. The significantly improved mechanical and electrical properties of cross-linked U-CNT (CL-U-CNT) fibers clearly indicated that the infiltration and cross-linking of urushiol is a straightforward and efficient strategy to ameliorate the performance of CNT fibers. The plausible reinforcement mechanism was also provided on the basis of the systematic structural characterization.

Experimental

Synthesis of CNT fibers

CNT fibers were synthesized and spun by the floating catalyst CVD (FCCVD) method. The detailed process was reported in our previous publication.²⁰

Extraction of urushiol

Urushiol was extracted from raw lacquer by using acetone as a solvent. Lacquer was mixed with acetone (1:3 volume ratio) and stored at room temperature for 24 hours without agitation. The mixed solution was naturally separated into the soluble portion containing urushiol and insoluble precipitates. The excess acetone was removed by using a rotary evaporator at 60 °C under reduced pressure to obtain urushiol. The obtained urushiol was a dark brown liquid and its chemical structure was characterized by using Fourier transform infrared (FT-IR) spectroscopy.

Reinforcement of CNT fibers by using urushiol

Urushiol was dissolved in N,N-dimethylformamide (DMF) by sonication at room temperature for 10 min. The prepared CNT fibers were immersed in the DMF solution of urushiol (1.0 mg mL⁻¹) for 10 min, taken out, and then exposed to a UV light source with a distance of 20 cm (365 nm, 1 kW) for 30 min. Finally, the UV treated CNT fibers were washed with DMF and dried in a vacuum oven overnight. As a control, pristine CNT fibers were treated using the same processes, except the presence of urushiol.

Characterization

The tensile mechanical properties of all tested CNT fibers were measured with a gauge length of 20 mm and a loading rate of 2 mm min⁻¹ by using a Textechno FAVIMAT equipped with a 0-2 N load cell providing a resolution of 10⁻⁶ N. The tensile experiment for each CNT fiber was repeated at least 20 times to obtain the statistically valid data. The electrical conductivities of all tested CNT fibers were measured with a four-point probe method by using a Keithley 2000E. The measurement of electrical conductivity was also performed at least 10 times for each CNT fiber to obtain the statistically valid data. The microstructure of CNT fibers was observed by using SEM (NOVA NanoSEM 450, FEI Co., The Netherlands). The cross-sectional areas of CNT fibers were calculated through analysing their crosssectional SEM images (Helios NanoLab 650 dual-beam focused ion beam, FEI Co., The Netherlands) by using ImageI software and dividing by the cosine of the tilt angle (30°). The structural changes of CNT fibers were analysed by using Raman spectroscopy (HORIBA LabRAM HR UV/Vis/NIR, Jobin Yvon, France).

Results and discussion

CNT fibers were synthesized and directly spun from a vertical CVD reactor continuously fed with a solution containing toluene, ferrocene, and thiophene which play roles as a carbon source, catalyst, and promoter, respectively. 20 The diameter of the as-spun CNT fibers was around 106 µm, and they exhibited a porous structure composed of numerous voids and entangled bundles of CNTs (Fig. 2a). These structural characteristics of CNT fibers are matched with a previous report and render their performance unsatisfactory for practical applications. 9-11 The asspun CNT fibers exhibited a tensile strength of 430 \pm 20 MPa, tensile modulus of 8.6 \pm 1.0 GPa, toughness of 12.7 \pm 1.3 MJ m⁻³, and electrical conductivity of 1616 \pm 115 S cm⁻¹ which are

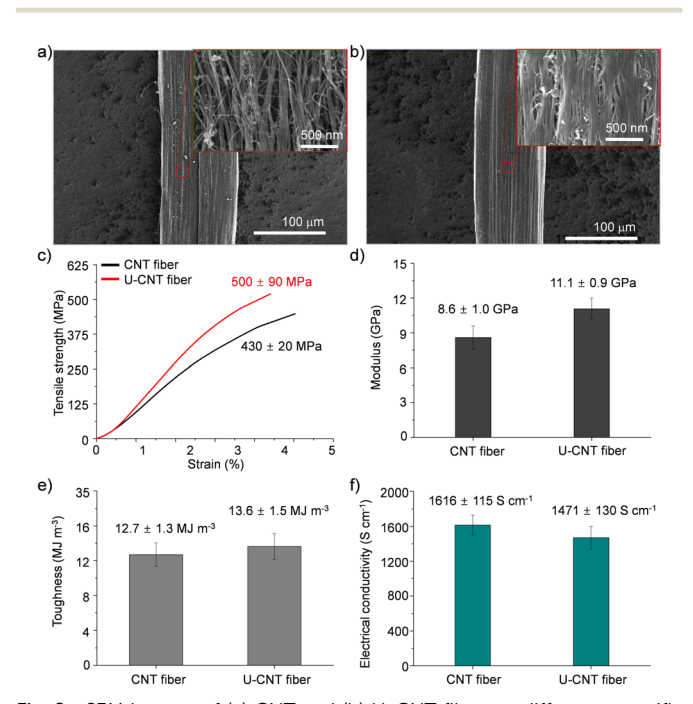


Fig. 2 SEM images of (a) CNT and (b) U-CNT fibers at different magnifications. (c) Tensile strength, (d) modulus, (e) toughness, and (f) electrical conductivity of CNT and U-CNT fibers.

inferior to the reported mechanical properties of individual CNTs (Fig. 2c-f).1 The CNT fibers were immersed in a DMF solution of urushiol for 10 min to induce infiltration of urushiol into their porous structures. After the infiltration, the diameter of the CNT fibers only slightly decreased to 102 µm, and their bundled structures became smooth with diminishing porous structures (Fig. 2b). This infiltration led to a slight enhancement of their tensile strength, modulus, and toughness to 500 \pm 90 MPa, 11.1 \pm 0.9 GPa, and 13.6 \pm 1.5 MJ m⁻³, respectively (Fig. 2c-e). By contrast, their electrical conductivity slightly decreased to $1471 \pm 130 \text{ S cm}^{-1}$ (Fig. 2f). There was almost no influence of DMF incubation on the mechanical properties of CNT fibers without urushiol (Fig. S1 in the ESI,† and see Fig. S2 for the optimization of urushiol concentration to be efficiently infiltrated into CNT fibers). These changes in the structure and properties implied that urushiol was successfully infiltrated into the porous structure of CNT fibers, and it facilitated the load transfer between CNT bundles through its π - π stacking while impeding the electron transfer between CNT bundles owing to its electrically insulating properties.

Then, the cross-linking effect of urushiol-infiltrated CNT (U-CNT) fibers was explored with both thermal and photochemical cross-linking processes. Urushiol contains unsaturated C-C bonds which can be efficiently cross-linked at high temperatures or under UV irradiation. 17,18 U-CNT fibers were heated to 300 °C for 1 h for thermal cross-linking of the infiltrated urushiol into CNT fibers to interlock CNT bundles consisting of CNT fibers through covalent bonds.^{7,17} The diameter of thermally cross-linked U-CNT (TC-U-CNT) fibers was around 77 µm which is much smaller than that of U-CNT fibers (Fig. 3a). This decrease intimated that the density of U-CNT fibers increased with the thermal cross-linking process. The high density is one of the most important features of a high-performance CNT fiber because the highly densified structure of the CNT fiber facilitates the load and electron transfer between CNT bundles consisting of CNT fibers.9 However, it is noteworthy that, while the U-CNT fibers were densified with the thermal cross-linking process, the internal structure of TC-U-CNT fibers became more porous than that of U-CNT fibers (Fig. 3a). This structural transition suggested that the thermal treatment of U-CNT fibers resulted in crosslinking of urushiol, accompanied by their thermal shrinkage and gasification. The thermal shrinkage and gasification of urushiol was examined by thermal treatment of urushiol (10 mg) on a Si substrate. The weight of urushiol decreased to 7.36 mg with phase transition from liquid to solid, and it was also confirmed that the weight of U-CNT fibers (2.482 mg) decreased by 10.24% after thermal cross-linking. Based on this structural transition, TC-U-CNT fibers exhibited considerable reinforcement of overall mechanical properties as well as electrical conductivity. Their tensile strength, modulus, toughness, and electrical conductivity increased to 0.92 \pm 0.09 GPa, 21.3 \pm 3.9 GPa, 20.5 \pm 2.3 MJ m⁻³, and 7430 \pm 447 S cm⁻¹, respectively (Fig. 3c-f). The properties are much better than those of CNT and U-CNT fibers, indicating that the thermal cross-liking facilitated the load and electron transfer between CNT bundles.

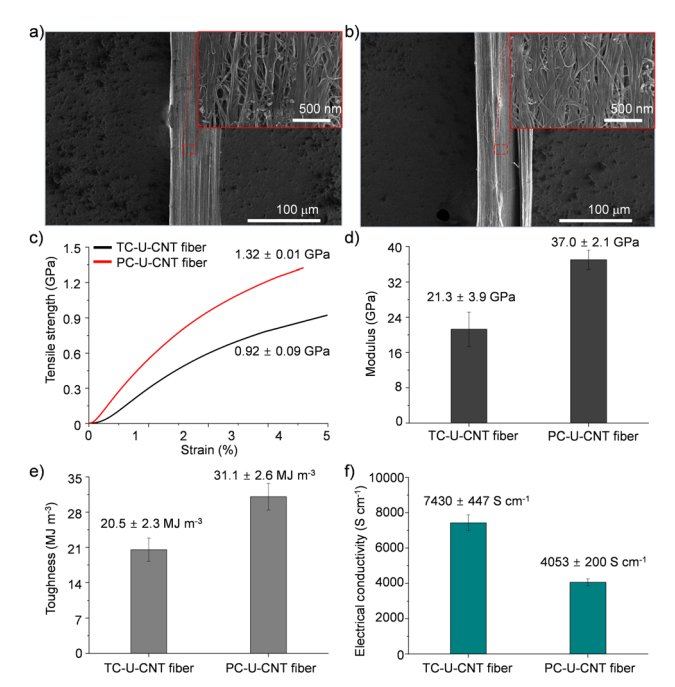


Fig. 3 SEM images of (a) TC-U-CNT and (b) PC-U-CNT fibers. (c) Tensile strength, (d) modulus, (e) toughness, and (f) electrical conductivity of TC-U-CNT and PC-U-CNT fibers.

Then, U-CNT fibers were exposed to an UV light source for photochemical cross-linking of the infiltrated urushiol to covalently interlock CNT bundles consisting of CNF fibers. After UV treatment, the diameter of photochemically crosslinked U-CNT (PC-U-CNT) fibers was around 77 µm comparable to that of TC-U-CNT fibers (Fig. 3b), but their internal structure was highly integrated with a diminished porous structure compared to CNT (Fig. 2a), U-CNT (Fig. 2b), and TC-U-CNT fibers (Fig. 3a). These results showed that the photochemical cross-linking of U-CNT fibers resulted in a more densified structure than thermal cross-linking. As expected from their highly densified structure, the tensile strength, modulus, toughness, and electrical conductivity of PC-U-CNT fibers were measured to be 1.32 \pm 0.01 GPa, 37.0 \pm 2.1 GPa, 31.1 \pm 2.6 MJ m⁻³, and 4053 \pm 200 S cm⁻¹, respectively (Fig. 3c-f). The mechanical properties of PC-U-CNT fibers were better than those of TC-U-CNT fibers, whereas their electrical conductivity was lower than that of TC-U-CNT fibers (Fig. S3, ESI,† for optimization of the UV irradiation time to efficiently cross-link U-CNT fibers). These results might be interpreted from the different internal structures of TC-U-CNT and PC-U-CNT fibers. TC-U-CNT fibers presented equally densified but highly porous structures compared to PC-U-CNT fibers. This structural difference signified that there was more residual urushiol on PC-U-CNT fibers than on TC-U-CNT fibers, and thus the residual urushiol on PC-U-CNT fibers led to more efficient mechanical reinforcement but less effective electron transfer. The amount of residual urushiol in TC-U-CNT and PC-U-CNT fibers was examined by measuring their weight changes induced by cross-linking treatments. After photochemical cross-linking, the weight of U-CNT fibers (2.474 mg) decreased by only 1.86%, and this weight decrease was much

lower than that caused by thermal cross-linking (10.24%). The slight weight difference of U-CNT fibers originated from the different initial weights of CNT fibers as well as the loading amount of urushiol. The average weight of CNT fibers (30 cm in their length) was 2.330 \pm 0.034 mg, and the average weight increase of CNT fibers was 7.53 \pm 0.29% by urushiol infiltration.

As a control, CNT fibers were simultaneously treated under thermal and photochemical cross-linking conditions. It was found that their mechanical and electrical properties were not nearly affected (Fig. S4, ESI†) and their weights decreased by only 1.0% after thermal treatment and 0.8% after photochemical treatment. This result clearly confirmed that urushiol played a pivotal role in the improvement of the mechanical and electrical properties of CNT fibers. It is also important that the performance of CNT fibers can vary depending on the crosslinking method: thermal cross-linking led to high electrical conductivity, whereas photochemical cross-linking resulted in good mechanical properties. To clarify the reinforcement effect of CNT fibers, the effect of their reduced diameter needs to be examined because the highly reduced diameter of CNT fibers can lead to apparent reinforcement of mechanical properties without an obvious increase of load transfer efficiency. The load value of CNT fibers (22.0 \pm 1.0 cN) increased to 26.7 \pm 0.7 cN by urushiol infiltration (Fig. S5, ESI†). After thermal and photochemical cross-linking, the load values of U-CNT fibers increased to 33.0 \pm 3.0 and 36.0 \pm 1.5 cN, respectively, but those of CNT fibers decreased to 21.6 \pm 1.2 and 13.7 \pm 1.2 cN by the simultaneous thermal and photochemical treatment (Fig. S5, ESI†). These results showed that the reinforcement of CNT fibers did not originate from their simply reduced crosssectional area but their enhanced load transfer efficiency.

The fracture analyses of CNT, U-CNT, TC-U-CNT, and PC-U-CNT fibers were carried out to examine the interlocking effect of infiltration and cross-linking of urushiol onto CNT fibers. The typical hairy-type failure was observed from the CNT fibers (Fig. 4a).¹³ This fracture behaviour indicated that the failure occurs by sliding of individual CNTs consisting of the CNT fibers when the applied shear force exceeds their friction force. The sliding of individual CNTs might start at a void and/ or at the end of the CNT bundles where the applied stress was concentrated. The U-CNT fibers showed a much less hairy-type structure at its fracture surface than the CNT fibers (Fig. 4b), which was ascribed to the interlocking effect of infiltrated urushiol. UC-U-CNT and PC-U-CNT fibers exhibited nearly no hairy-type structure at their fracture surfaces (Fig. 4c and d), and this failure behaviour implied that both thermal and photochemical cross-linking processes substantially reinforced the interaction between CNT bundles which restricted sliding of individual CNTs rather than their collective fracture.

To investigate the structural influence of urushiol crosslinking on the chemical structures of CNT fibers, CNT, U-CNT, TC-U-CNT, and PC-U-CNT fibers were then characterized by Raman spectroscopy. The Raman spectrum of CNT fibers showed typical G- and D-peaks at 1573 and 1345 cm⁻¹ which are derived from the vibrational transitions of their ordered and disordered sp² carbon structures, respectively (Fig. 5a).⁷

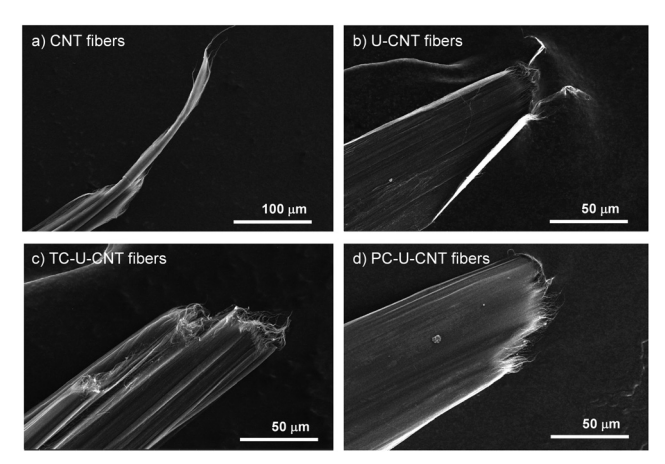


Fig. 4 Fractographic SEM images of (a) CNT, (b) U-CNT, (c) TC-U-CNT, and (d) PC-U-CNT fibers.

The relative intensity ratio of G- and D-peaks $(I_{\rm G}/I_{\rm D})$ has been used as an indicator of the degree of defects on CNT fibers. The $I_{\rm G}/I_{\rm D}$ value of CNT fibers was 3.0 \pm 0.2, and it slightly decreased to 2.9 \pm 0.1 by infiltration of urushiol (Fig. 5a and b). This result suggested that the infiltrated urushiol was not covalently bonded but physically adsorbed on the surface of CNT fibers. After thermal cross-linking, the $I_{\rm G}/I_{\rm D}$ value of U-CNT fibers became 2.8 \pm 0.1 which was comparable to their initial value (Fig. 5a and b). By stark contrast, the $I_{\rm G}/I_{\rm D}$ value of PC-U-CNT fibers substantially decreased to 2.6 \pm 0.3 by photochemical cross-linking, suggesting photochemical cross-linking resulted

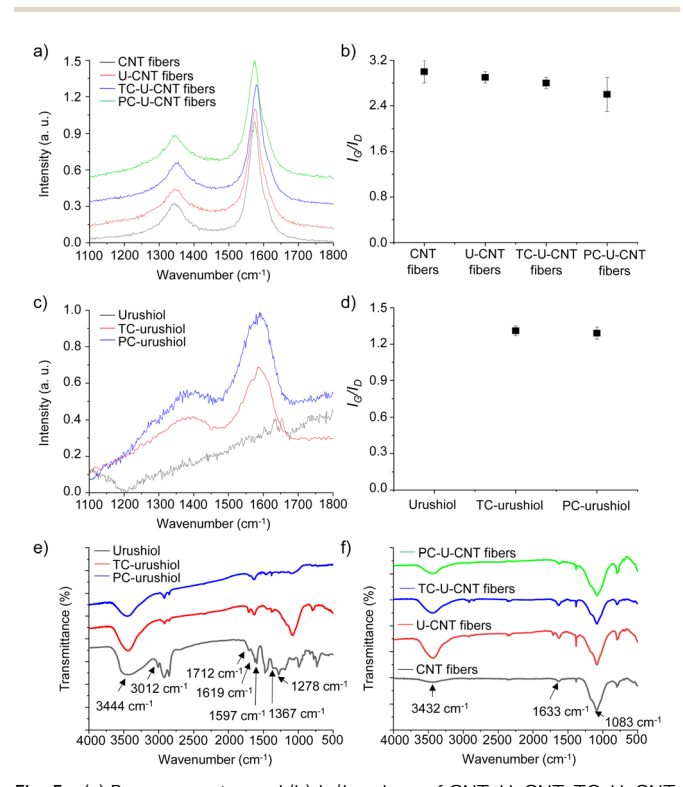


Fig. 5 (a) Raman spectra and (b) $I_{\rm G}/I_{\rm D}$ values of CNT, U-CNT, TC-U-CNT, and PC-U-CNT fibers. (c) Raman spectra and (b) $I_{\rm G}/I_{\rm D}$ values of urushiol, UC-urushiol, and PC-urushiol.

in formation of defects (Fig. 5a and b). As a control to clearly demonstrate the structural transition with the cross-linking process, CNT fibers were also treated simultaneously under thermal and photochemical cross-linking conditions, except urushiol infiltration. The I_G/I_D value of CNT fibres was enhanced to 3.5 \pm 0.1 by thermal treatment but only slightly increased to 3.1 \pm 0.1 by photochemical treatment (Fig. S6a and b, ESI \dagger). The changes of the I_G/I_D value showed that the thermal treatment highly improved the crystallinity of CNT fibers compared to photochemical treatment. These results are well matched with our previous reports.7 Considering the control results, both cross-linking processes introduced many defects in CNT fibers. However, the thermal treatment can further compensate for the deterioration of crystallinity induced by the thermal cross-linking reaction, and thus the I_G/I_D value of TC-U-CNT fibers was higher than that of PC-U-CNT fibers after cross-linking treatment.

In addition to the mechanical properties, the electrical conductivity of CNT fibers was also enhanced with infiltration and subsequent cross-linking of urushiol. It is interesting because the infiltration of urushiol into CNT fibers decreased their electrical conductivity despite its densification effect, implying that urushiol acted as an insulating layer. Thus, the increased electrical conductivity of U-CNT fibers by crosslinking suggested that the chemical structures of the infiltrated urushiol might be changed during the cross-linking processes. To examine the structural changes of urushiol upon both thermal and photochemical cross-linking treatments, urushiol was coated on a silicon wafer, then treated under high temperature and UV irradiation, and analysed by Raman spectroscopy. As expected, no signal was detected from the as-coated urushiol (Fig. 5c), but after both thermal and photochemical treatments, the typical D- and G-peaks of graphitic materials were observed at 1384 and 1585 cm⁻¹, respectively (Fig. 5c and d). The evolution of D- and G-peaks indicated that there was a partial carbonization of urushiol under both cross-linking treatments. The I_G/I_D values of thermally and photochemically cross-linked urushiol (TC-urushiol and PC-urushiol) were 1.32 ± 0.03 and 1.28 ± 0.04 , respectively, which suggested that the thermal cross-linking led to more efficient carbonization than photochemical cross-linking. This difference in the degree of carbonization might be another origin of the higher electrical conductivity of TC-U-CNT fibers than that of PC-U-CNT fibers. The Raman spectroscopy analyses clearly revealed the improved electrical conductivity of CNT fibers by urushiol infiltration and cross-linking treatments, which was attributed to both the densification effect and partial carbonization of the infiltrated urushiol.

To further confirm the cross-linking of urushiol on the surface of CNT fibers, the structural changes in urushiol induced by thermal and photochemical treatments were analysed by FT-IR spectroscopy. The FT-IR spectrum of urushiol exhibited broad peaks at 3444 cm⁻¹ from the O-H stretching vibration, 3012 cm⁻¹ from the C-H stretching vibration of unsaturated C-C bonds in side changes, 1712 cm⁻¹ from the C-O stretching vibration, and 1619 and 1597 cm⁻¹ from

the vibration of the phenyl ring (Fig. 5e).²¹ After thermal and photochemical cross-linking, the intensity of the O-H stretching vibration decreased and the C-H stretching vibration of unsaturated C=C bonds disappeared due to the partial removal of the hydroxyl groups on phenyl rings and the crosslinking of side chains, respectively (Fig. 5e). In addition, the C=O stretching vibration also decreased with cross-linking (Fig. 5e). These changes are well matched with a previous report and indicated that urushiol was successfully crosslinked under our experimental conditions.²¹ Then, CNT, U-CNT, TC-U-CNT, and PC-U-CNT fibers were also characterized by FT-IR spectroscopy. The FT-IR spectrum of CNT fibers showed typical peaks at 1085 cm⁻¹ from the C-O stretching vibration, 1633 cm⁻¹ from the aromatic C=C stretching vibration, and 3432 cm⁻¹ from the O-H stretching vibration (Fig. 5f). It was previously reported that the surface of CNT fibers was partially oxidized because they were synthesized in a vertical CVD reactor with an open atmosphere.²² By urushiol infiltration, the peak of O-H stretching vibration was enhanced, and several new peaks appeared at 1710 and 1382 cm⁻¹ which originated from the C=O stretching vibration and C-O-H bending vibration, respectively (Fig. 5f). Similar to the changes in urushiol by cross-linking treatments, the FT-IR spectra of TC-U-CNT and PC-U-CNT fibers exhibited a decrease in C-O-H bending, O-H and C=O stretching vibration peaks, and it is also worth noting that the degree of decrease was higher on PC-U-CNT fibers than on TC-U-CNT fibers, implying that the cross-linking of U-CNT fibers was more efficient with photochemical cross-linking than with thermal cross-linking (Fig. 5f, and for further characterization by XPS, see Fig. S7, ESI†). These results are well correlated with the results of Raman analysis.

Conclusions

In summary, we demonstrated a simple and efficient strategy to concurrently enhance the mechanical and electrical properties of CNT fibers by infiltration and cross-linking of urushiol. Urushiol was readily infiltrated into CNT fibers and crosslinked by thermal and photochemical treatments. The tensile strength (430 \pm 20 MPa), modulus (8.6 \pm 1.0 GPa), toughness (12.7 \pm 1.3 MJ m⁻³), and electrical conductivity (1616 \pm 115 S cm⁻¹) of CNT fibers were substantially enhanced to 1.32 ± 0.01 GPa, 37.0 ± 2.1 GPa, 31.1 ± 2.6 MJ m⁻³, and $4053 \pm 200 \, \mathrm{S \, cm^{-1}}$ with photochemical treatment and to 0.92 \pm 0.09 GPa, 21.3 \pm 3.9 GPa, 20.5 \pm 2.3 MJ m $^{-3}$, and 7430 \pm 447 S cm⁻¹ with thermal treatment, respectively. These enhanced properties of CNT fibers by infiltration and cross-linking of urushiol were derived from its densification, increased interfacial interaction through covalent bonds, and partial carbonization. Taking together the simplicity and high efficiency, we believe this strategy will be a practical, eco-friendly, and important way to develop high-performance CNT fibers for applications in automobile, electrical conductor, defence, and aerospace industries.

Author contributions

Hyun Jun Cho: conceptualization, data curation, methodology, writing - review & editing. Chul-Jun Yoon: conceptualization, data curation, methodology. Junbeom Park: resources, data curation. Hansol Kang: resources. Insik In: resources, writing - original draft. Seung Min Kim: conceptualization, funding acquisition, supervision, writing - original draft. Young-Kwan Kim: conceptualization, data curation, methodology, formal analysis, investigation, funding acquisition, supervision, writing - original draft, writing - review & editing.

Conflicts of interest

There are no conflicts to declare.

Acknowledgements

This work was supported by the National Research Foundation of Korea (NRF) grant funded by the Korea government, Ministry of Science and ICT (MSIT) (No. 2022R1C1C1008388). This work was also supported by grants from the Korea Institute of Science and Technology Open Research Program (2E31901) and the Technology Innovation Program (20017548) funded by the Ministry of Trade, Industry & Energy (MOTIE, Korea). This research was supported by the Basic Science Research Program through the National Research Foundation of Korea (NRF) funded by the Ministry of Education (2022R1A6A 1A03053343).

References

- 1 M. F. Yu, O. Lourie, M. J. Dyer, K. Moloni, T. F. Kelly and R. S. Ruoff, Science, 2000, 287, 637.
- 2 N. Behabtu, M. J. Green and M. Pasquali, Nano Today, 2008,
- 3 Y. Li, I. A. Kinloch and A. H. Windle, Science, 2004, 304, 276.
- 4 N. Behabtu, C. C. Younh, D. E. Tsentalovich, X. Wang, A. W. Ma, E. A. Bengio, R. F. ter Waarbeek, J. J. de Jong, R. E. Hoogerwerf, S. B. Fairchild, J. B. Ferguson, B. Maruyama, J. Kono, Y. Talmon, Y. Cohen, M. J. Otto and M. Pasquali, Science, 2013, 339, 182.
- 5 M. Zhang, K. R. Atkinson and R. H. Baughman, Science, 2004, 306, 1358.
- 6 S.-H. Lee, J. Park, H.-R. Kim, J. Lee and K.-H. Lee, RSC Adv., 2015, 5, 41894.
- 7 Y.-K. Kim, Y.-J. Kim, J. Park, S. W. Han and S. M. Kim, Carbon, 2021, 173, 376.
- 8 W. Xu, Y. Chen, H. Zhan and J. N. Wang, Nano Lett., 2016,
- 9 J. Lee, D.-M. Lee, Y. Jung, J. Park, H. S. Lee, Y.-K. Kim, C. R. Park, H. S. Jeong and S. M. Kim, Nat. Commun., 2019,
- 10 Y.-J. Kim, J. Park, H. S. Jeong, M. Park, S. Baik, D. S. Lee, H. Rho, H. Kim, J. H. Lee, S. M. Kim and Y.-K. Kim, Nanoscale, 2019, 11, 5295.

- 11 T. Kim, J. Shin, K. Lee, Y. Jung, S. B. Lee and S. J. Yang, *Composites, Part A*, 2021, **140**, 106182.
- 12 S. Ryu, J. B. Chou, K. Lee, D. Lee, S. H. Hong, R. Zhao, H. Lee and S.-G. Kim, *Adv. Mater.*, 2015, 27, 3250.
- 13 Y.-J. Kim, J. Park, H. Kim, H. S. Jeong, J. H. Lee, S. M. Kim and Y.-K. Kim, *Compos. B. Eng.*, 2019, **163**, 431.
- 14 H. Watanabe, A. Fujimoto, J. Nishida, T. Ohishi and A. Takahara, *Langmuir*, 2016, 32, 4619.
- 15 H. Watanabe, A. Fujimoto and A. Takahara, J. Polym. Sci., Part A: Polym. Chem., 2013, 51, 3688.
- 16 S. Ryu, Y. Lee, J.-W. Hwang, S. Hong, C. Kim, T. G. Park, H. Lee and S. H. Hong, *Adv. Mater.*, 2011, 23, 1971.

- 17 H. Watanabe, A. Fujimoto and A. Takahara, *ACS Appl. Mater. Interfaces*, 2014, **6**, 18517.
- 18 J. Xia, J. Lin, Y. Xu and Q. Chen, ACS Appl. Mater. Interfaces, 2011, 3, 482.
- 19 B.-C. Shiu, K. Wu, C.-W. Lou, Q. Lin and J.-H. Lin, *Polymers*, 2021, **13**, 2858.
- 20 S.-H. Lee, H.-R. Kim, H. Lee, J. Lee, C.-H. Lee, J. Lee, J. Park and K.-H. Lee, *Chem. Eng. Sci.*, 2018, **192**, 655.
- 21 J. Xia, J. Lin, Y. Xu and Q. Chen, ACS Appl. Mater. Interfaces, 2011, 3, 482.
- 22 C.-J. Yoon, S.-H. Lee, Y.-B. Kwon, K. Kim, K.-H. Lee, S. Min Kim and Y.-K. Kim, *Appl. Surf. Sci.*, 2021, **541**, 148332.